Anti-Stokes emissions and determination of Stark sub-level diagram of Er^{3+} ions in KY_3F_{10}

2006 J. Phys.: Condens. Matter 18 6721

(http://iopscience.iop.org/0953-8984/18/29/012)

INSTITUTE OF PHYSICS PUBLISHING JOURNAL OF PHYSICS: CONDENSED MATTER

J. Phys.: Condens. Matter **18** (2006) 6721–6727 doi:10.1088/0953-8984/18/29/012

Anti-Stokes emissions and determination of Stark sub-level diagram of Er^{3+} ions in KY_3F_{10}

E Boulma[1,2], M Diaf[2], J P Jouart[1], M Bouffard[1], J L Doualan[3] and R Moncorgé[3]

[1] Laboratoire d'Energétique et d'Optique, UTAP, Université de Reims Champagne-Ardenne, BP 1039, Reims Cedex 51 687, France

[2] Département de Physique, Université Badji Mokhtar Annaba, BP12, 23000 Annaba, Algérie

[3] Centre Interdisciplinaire de Recherches Ions Lasers (CIRIL), UMR 6637 CNRS-CEA-ISMRA, ENSI de Caen, 6 Boulevard Maréchal Juin, 14050 Caen Cedex, France

Received 15 March 2006, in final form 23 May 2006
Published 30 June 2006
Online at stacks.iop.org/JPhysCM/18/6721

Abstract

We are interested, in this work, in determining the Stark sub-level of Er^{3+} ions doping a KY_3F_{10} single crystal with a molar concentration of 1%. We have used a new method of measurement of energies of the ground level and emitting levels from excitation and anti-Stokes emission spectra recorded at liquid nitrogen temperature. This technique is based on a spectral analysis of the anti-Stokes emissions recorded after selective excitation with a red dye tunable laser. Thus, we could determine the Stark sub-levels of the ground and the principal emitting levels in the infrared, visible and near-UV ranges with a very good precision.

1. Introduction

Research in the field of solid state lasers has not ceased increasing from one year to the next. Solid state laser materials doped with trivalent rare earth ions increasingly attract the researchers' attention. In order to produce high power lasers, these material hosts, used as single crystals or glasses, must have interesting mechanical properties, a rather broad range of transparency and rather high threshold optical damage. Fluoride materials containing trivalent ions, mainly Y^{3+} cations, are very advantageous because they can be substituted easily by rare earth ions of the same valence. Moreover, the fluoride materials compared with oxides have low phonon energies that makes it possible to reduce the nonradiative deexcitation phenomena by multiphonon emissions, thus ensuring good fluorescence quantum yields for the principal emitting levels. They also have a reasonably high thermal conductivity compared to chlorides and bromides known as having very low phonon energies, which supposes that they have good thermomechanical properties and a high chemical stability.

For all these reasons, the compound KY_3F_{10} of the KF–YF_3 pseudo-binary system has been the subject of many studies especially in the spectroscopic and magnetic fields during these few last years [1–11]. It presents a good number of advantages for the study of the optical processes brought into play to reach the spectral range 1.5–3 μm which is very interesting for many applications [12–15]. Indeed, it is a congruent compound with a not very high melting point (1030 °C) [16], and thus is relatively easy to synthesize as a single crystal. It crystallizes in the fluorite type of cubic structure, belonging to the space group $Fm3m$ [17]. The lattice is made up of two ionic groups $(KY_3F_8)^{2+}$ and $(KY_3F_{12})^{2-}$ which are alternated along orthogonal crystallographic directions [18, 19]. In the first group, the F^- ions occupy the tops of an empty cube inside the first sub-lattice. In the second, they form an empty cubooctahedron. The Y^{3+} ions, for which are partially substituted the Er^{3+} ions, occupy a tetragonal symmetry site (C_{4v}). Compared to other well-known fluoride laser crystals like $LiYF_4$ or BaY_2F_8, its crystal structure tolerates a large lanthanide concentration. It has a rather broad range of transparency (0.2–8 μm). Moreover, it has a rather strong crystal field leading to a high splitting of the energy levels for the rare earth and in particular for the ground level as in the case of thulium doping [4].

In this work, we are interested in exploring the results of a spectral analysis of the anti-Stokes emissions for Er^{3+} ions incorporated in a KY_3F_{10} crystal by using a selective excitation technique around 650 nm provided by a tunable laser. This study permits us to determine the Stark sub-levels of the various ${}^{2S+1}L_J$ excited multiplets and the ground multiplet of Er^{3+} ion with a very good precision [20].

2. Experiment

Er^{3+} (1%) doped KY_3F_{10} single crystals were synthesized by the Czochralski pulling technique under highly purified argon atmosphere using a carbon–vitreous crucible. The starting compounds containing yttrium or rare-earth fluoride YF_3 and ErF_3 were purified by a fluoridation reaction such as that presented by Gesland [21]. The single crystals obtained were of good optical quality, not diffusing He–Ne laser light.

The emission spectra were recorded at liquid nitrogen temperature under continuous excitation (into the ${}^4F_{9/2}$ multiplet) provided by a dye laser (Kiton-Red) tunable from 620 to 660 nm and pumped by a CW multiline mode argon laser (Spectra Physics).

The pump laser beam, having a 500 mW output power, is focused with a lens of 30 cm focal distance on the unoriented sample placed on the cold finger of a liquid nitrogen cryostat. The fluorescence induced in the range from 11 500 to 22 500 cm^{-1} is analysed by a Coderg T800 three-grating monochromator and then detected by a water-cooled photomultiplier (EMI 9558QB). The excitation spectra are also recorded by continuous variation of the wavelength of the dye laser from 620 to 660 nm through absorption corresponding to the ${}^4I_{15/2} \rightarrow {}^4F_{9/2}$ erbium transition. The emission and excitation spectrum lines are positioned with a precision of ± 1 cm^{-1}.

For decay measurements, the laser beam is switched off by an electro-optic modulator, and an oscillograph (Tektronix TDS 210) interfaced with a microcomputer is used to record the decay of luminescence.

3. Results

The emission spectrum of the Er^{3+} ions incorporated in KY_3F_{10} crystal was recorded at liquid nitrogen temperature in the spectral range from 11 500 to 22 500 cm^{-1} under continuous excitation in the ${}^4F_{9/2}$ multiplet at 15 366 or 15 457 cm^{-1}. The total spectrum is composed of several groups of lines. Referring to the literature related to the Er^{3+} ions [22], we have identified many transitions including, in particular, the following ones (figure 1):

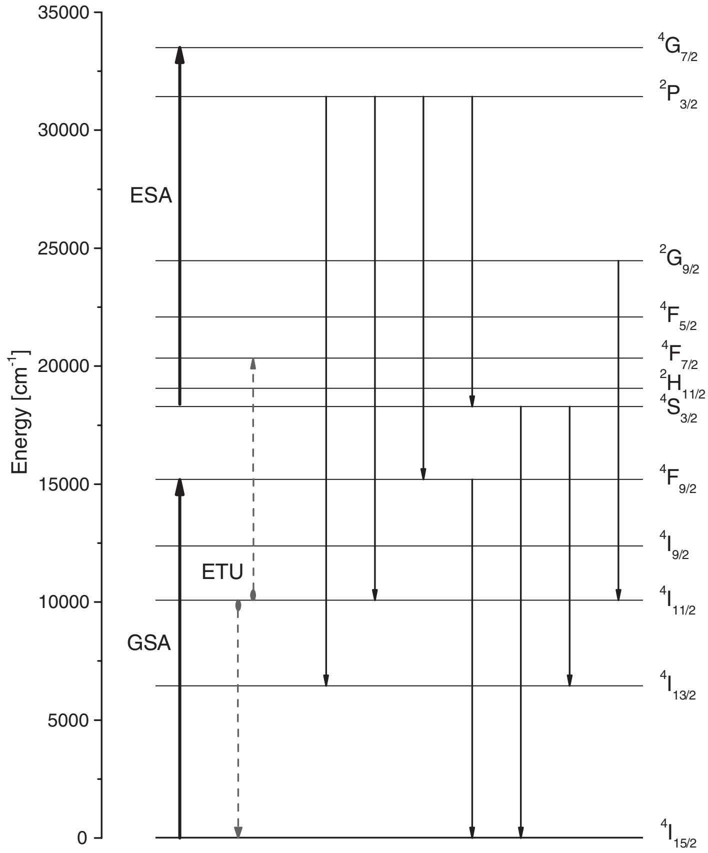

Figure 1. Excitation mechanisms and Er^{3+} anti-Stokes transitions studied to determine the Stark sub-levels.

- four anti-Stokes transitions coming from the $^2P_{3/2}$ multiplet ($^2P_{3/2} \rightarrow {}^4S_{3/2}$, $^4F_{9/2}$, $^4I_{11/2}$ and $^2P_{3/2} \rightarrow {}^4I_{13/2}$ in the second order);
- two anti-Stokes transitions coming from the $^4S_{3/2}$ multiplet ($^4S_{3/2} \rightarrow {}^4I_{13/2}$, $^4I_{15/2}$);
- one anti-Stokes transition coming from the $^2G_{9/2}$ multiplet ($^2G_{9/2} \rightarrow {}^4I_{11/2}$);
- one Stokes transition ($^4F_{9/2} \rightarrow {}^4I_{15/2}$).

In the course of this study, three two-step emission processes (figure 1) have been specially exploited to determine the Stark sub-level diagram of Er^{3+}.

The absorption mechanism in the metastable states as well as the nonradiative energy transfers between the excited Er^{3+} ions contribute to populate the higher levels and give place to the transitions observed (figure 1), the energy transfer being predominant when the concentration in Er^{3+} ions is equal to or higher than 1% [23]. The slow component which we observed in the green ($^4S_{3/2} \rightarrow {}^4I_{15/2}$) emission decay suggests that the $^4S_{3/2}$ level is populated through an energy transfer upconversion (ETU) process involving two nearby Er^{3+} ions in the $^4I_{11/2}$ state (figure 1). The blue ($^2P_{3/2} \rightarrow {}^4I_{11/2}$) emission decay was fitted by a single exponential with a time constant of 0.31 ms. This emission is tentatively attributed to Er^{3+} ions excited in the $^2P_{3/2}$ state through an excited-state absorption (ESA) starting from $^4S_{3/2}$ (figure 1).

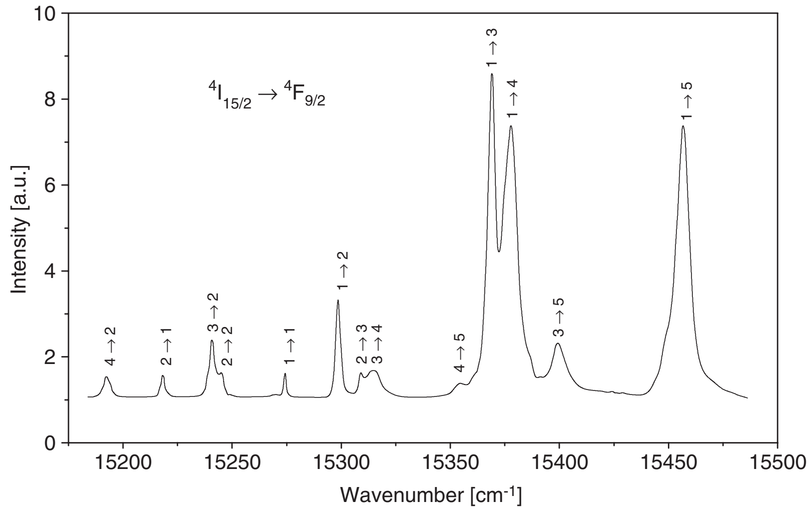

Figure 2. Excitation spectrum of the green emission of Er^{3+} (1%) in KY_3F_{10} at 77 K corresponding to the $^4I_{15/2} \rightarrow {}^4F_{9/2}$ transition.

The excitation spectrum of the red emission (14 983 cm^{-1}) or of the green emission (18 357 cm^{-1}) recorded between 15 200 and 15 500 cm^{-1} presents a dozen lines which we attribute to the $^4I_{15/2} \rightarrow {}^4F_{9/2}$ transition (figure 2). We attribute the line of this spectrum having the highest energy (15 457 cm^{-1}) to the transition between the basic sub-level of the ground state $^4I_{15/2}$ and the fifth sub-level of the $^4F_{9/2}$ multiplet ($^4I_{15/2}(1) \rightarrow {}^4F_{9/2}(5)$). We can then position the last Stark sub-level of $^4F_{9/2}$ at 15 457 cm^{-1}, $^4I_{15/2}(1)$ being taken as the energy reference mark.

The emission spectrum recorded in the spectral range 16 000–16 400 cm^{-1} is attributed to the transition between excited states $^2P_{3/2} \rightarrow {}^4F_{9/2}$ (figure 3(a)). The line of this spectrum having the lowest energy (16 098 cm^{-1}) corresponds to the $^2P_{3/2}(1) \rightarrow {}^4F_{9/2}(5)$ transition that allows us to position the first Stark sub-level of $^2P_{3/2}(1)$ to $15\,457 + 16\,098 = 31\,555$ cm^{-1}.

In addition, the blue emission spectrum recorded between 21 200 and 21 500 cm^{-1} contains 11 lines among 12 lines expected for the $^2P_{3/2} \rightarrow {}^4I_{11/2}$ transition (figure 3(b)). After having positioned all the lines observed, we located an energy difference equal, on average, to 98 cm^{-1} for six couples of lines. This split corresponds to the difference in energy between the only two $^2P_{3/2}$ sub-levels. This allows us to locate the second Stark sub-level of $^2P_{3/2}$ at $31\,555 + 98 = 31\,653$ cm^{-1}. On this same blue emission spectrum, the line having the highest energy (21 460 cm^{-1}) corresponds to the $^2P_{3/2}(2) \rightarrow {}^4I_{11/2}(1)$ transition and the associated line to the $^2P_{3/2}(1) \rightarrow {}^4I_{11/2}(1)$ transition. The position of the first $^4I_{11/2}$ sub-level is then equal to $31\,653\text{-}21\,460 = 10\,193$ cm^{-1}.

We proceed in the same manner with the remaining line couples to determine the other Stark sub-levels of $^4I_{11/2}$, which makes it possible to affirm that until this stage, $^2P_{3/2}$ and $^4I_{11/2}$ Stark sub-levels are determined in addition to the last sub-level $^4F_{9/2}$ multiplet.

On the infrared emission spectrum recorded between 13 000 and 13 350 cm^{-1} and corresponding to the transition $^2P_{3/2} \rightarrow {}^4S_{3/2}$ (figure 3(c)), we have located the line couples having the difference of 98 cm^{-1} to place the two $^4S_{3/2}$ sub-levels at 18 413 and 18 490 cm^{-1} according to the same protocol previously described for $^4I_{11/2}$. It is obvious that the knowledge of the $^2P_{3/2}$ sub-level positions, from which we have located four transitions in the first order,

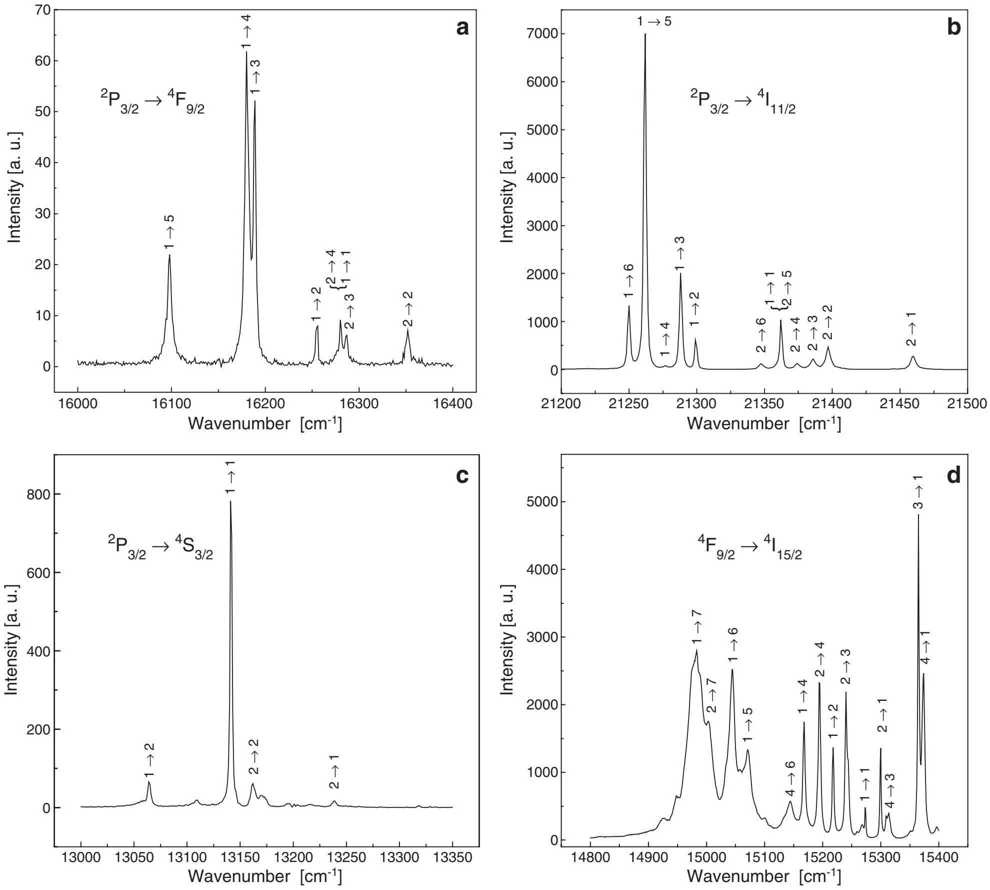

Figure 3. Anti-Stokes emission of Er^{3+} (1%) in KY_3F_{10} at 77 K corresponding to the transitions: (a) $^2P_{3/2} \rightarrow {}^4F_{9/2}$; (b) $^2P_{3/2} \rightarrow {}^4I_{11/2}$; (c) $^2P_{3/2} \rightarrow {}^4S_{3/2}$; the unidentified peaks are attributed to $^4G_{11/2} \rightarrow {}^4I_{15/2}$ (order 2). Stokes emission of Er^{3+} in KY_3F_{10} at 77 K corresponding to the transition: (d) $^4F_{9/2} \rightarrow {}^4I_{15/2}$. The intensity scales are independent.

facilitates the determination of the sub-level energies of the final levels. Following the same calculation method used up to now, we determined the four remaining $^4F_{9/2}$ sub-levels from the emission spectrum due to $^2P_{3/2} \rightarrow {}^4F_{9/2}$ transition. These positions are easily checked using the excitation spectrum of the red or green emission (figure 2).

We used the two red and green emission spectra corresponding respectively to the transitions $^4F_{9/2} \rightarrow {}^4I_{15/2}$ and $^4S_{3/2} \rightarrow {}^4I_{15/2}$ (figures 3(d) and 4(a)) to explore the $^4I_{15/2}$ ground Stark level structure of the Er^{3+} ions. The combination of the results obtained with these two spectra enabled us to determine the eight sub-levels of the $^4I_{15/2}$ multiplet at energies 0, 57, 61, 106, 203, 230, 293 and 338 cm^{-1}.

Until now, we have located the sub-levels of the $^4I_{15/2}$, $^4I_{11/2}$, $^4F_{9/2}$, $^4S_{3/2}$ and $^2P_{3/2}$ multiplets. The analysis of the spectrum corresponding to a transition for which one of two multiplets brought into play has its Stark structure given led us to the determination of the Stark structure of the other especially when there is not an overlapping of fluorescence. Thus, the $^4S_{3/2} \rightarrow {}^4I_{13/2}$ and $^2G_{9/2} \rightarrow {}^4I_{11/2}$ transitions (figures 4(b) and (c)) allowed us to locate the Stark sub-levels of $^4I_{13/2}$ and $^2G_{9/2}$ multiplets. The infrared emission spectrum recorded

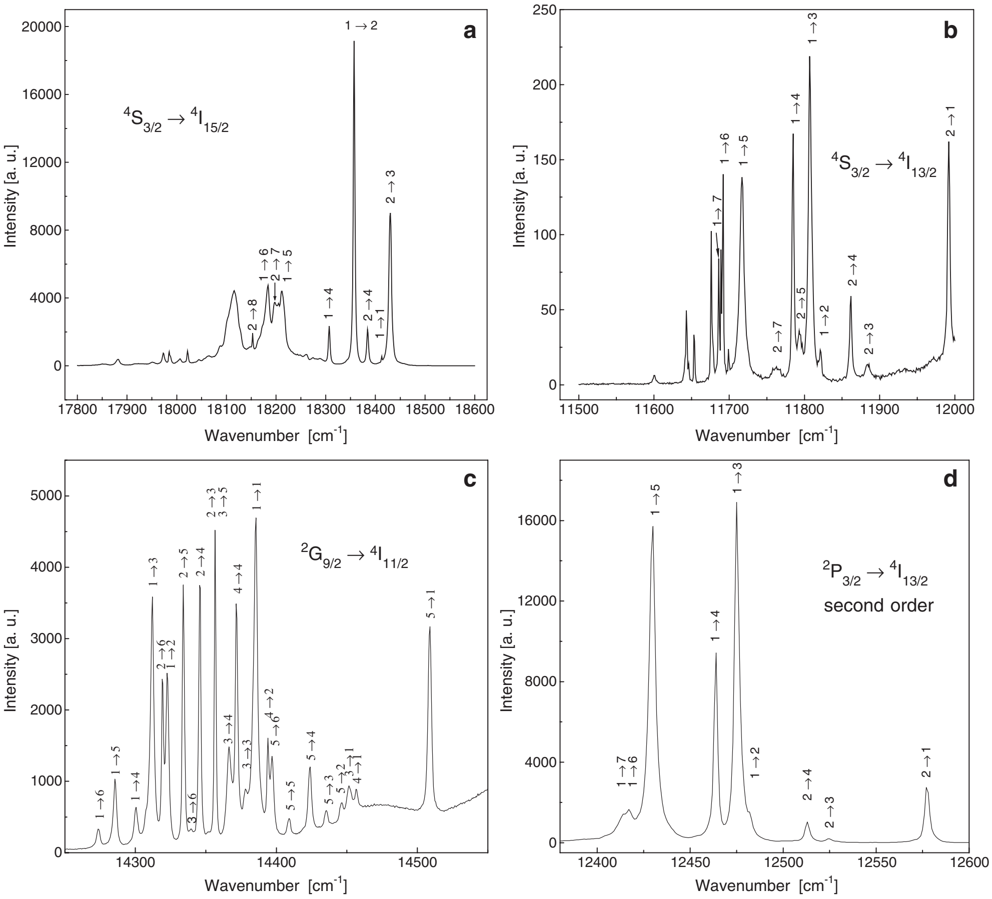

Figure 4. Anti-Stokes emission of Er^{3+} (1%) in KY_3F_{10} at 77 K corresponding to the transitions: (a) $^4S_{3/2} \rightarrow {}^4I_{15/2}$ (the unidentified peaks located below 18 050 cm^{-1} are attributed to $^2G_{9/2} \rightarrow {}^4I_{13/2}$); (b) $^4S_{3/2} \rightarrow {}^4I_{13/2}$ (the unidentified peaks located below 11 700 cm^{-1} are attributed to $^4D_{5/2} \rightarrow {}^4F_{9/2}$, second order); (c) $^2G_{9/2} \rightarrow {}^4I_{11/2}$; (d) $^2P_{3/2} \rightarrow {}^4I_{13/2}$. The intensity scales are independent.

Table 1. Stark sub-level energies of the Er^{3+} ions in KY_3F_{10}.

	Sub-levels energy (in cm^{-1})							
Multiplet	1	2	3	4	5	6	7	8
$^4I_{15/2}$	0	57	61	106	203	230	293	338
$^4I_{13/2}$	6 498	6 592	6 606	6 628	6 697	6 721	6 727	
$^4I_{11/2}$	10 193	10 256	10 267	10 279	10 291	10 305		
$^4F_{9/2}$	15 274	15 300	15 366	15 374	15 457			
$^4S_{3/2}$	18 413	18 490						
$^2G_{9/2}$	24 578	24 625	24 646	24 649	24 702			
$^2P_{3/2}$	31 555	31 653						

between 12 400 and 12 600 cm^{-1} corresponding to the $^2P_{3/2} \rightarrow {}^4I_{13/2}$ transition in the second order (figure 4(d)) enabled us to check the positions of the $^4I_{13/2}$ sub-levels. The determined Stark sub-level energies are summarized in table 1.

The use of this selective excitation technique gives energies with a precision of $\pm 1\ cm^{-1}$. The results obtained agree with those given by the literature [24–27] by using the usual method of combined analysis of the emission and absorption spectra.

4. Conclusion

We obtained, on a KY_3F_{10} single crystal doped by Er^{3+} ions with a molar concentration of 1%, emission spectra at liquid nitrogen temperature using the selective excitation technique. The analysis of these spectra, combined with those of the excitation, recorded at the same temperature, has enabled us to experimentally determine the Stark sub-level energy diagram of the Er^{3+} ion for seven multiplets.

References

[1] Porcher P and Caro P 1976 *J. Chem. Phys.* **65** 89
[2] Heyde K, Binnemans K and Görller-Walrand C 1998 *J. Chem. Soc., Faraday Trans.* **94** 1671
[3] Wells J P R, Sugiyama A, Han T P J and Gallagher H G 1999 *J. Lumin.* **85** 91
[4] Diaf M, Braud A, Labbé C, Doualan J L, Girard S, Margerie J, Moncorgé R and Thuau M 1999 *Can. J. Phys.* **77** 693
[5] Braud A, Girard S, Doualan J L, Thuau M and Moncorgé R 2000 *Phys. Rev.* B **61** 5280
[6] Yamaga M, Honda M, Wells J P R, Han T P J and Gallagher H G 2000 *J. Phys.: Condens. Matter* **12** 8727
[7] Braud A, Tigreat P Y, Doualan J L and Moncorgé R 2001 *Appl. Phys.* B **72** 909
[8] Tigreat P Y, Doualan J L, Budasca C and Moncorgé R 2001 *J. Lumin.* **94/95** 23
[9] Grzechnik A, Crichton W A and Gesland J Y 2003 *Solid State Sci.* **5** 757
[10] Silva E N, Ayala A P, Gesland J Y and Moreira R L 2005 *Vib. Spectrosc.* **37** 21
[11] Chamberlain S L and Corruccini L R 2005 *Phys. Rev.* B **71** 24434
[12] Brunetaud J M 1998 *Opt. Photon.* **3** 53
[13] Barnes N P 1995 *Laser Focus World* **31** 87
[14] Dineman B J and Moulton P F 1994 *Opt. Lett.* **19** 1143
[15] Wyss C, Lüthy W, Weber H P, Rogin P and Hulliger J 1997 *Opt. Commun.* **139** 215
[16] Chai B, Lefaucheur J, Pham A, Lutts G and Nichols J 1993 *Proc. SPIE* **1863** 131
[17] Pierce J W and Hong H Y P 1973 *Proc. 10th Rare Earth Conf. (Arizona)* p 114
[18] Mortier M, Gesland J Y, Rousseau M, Pimenta M A, Laderia L O, Machado J C, Silva D and Barbosa G A 1991 *J. Raman Spectrosc.* **22** 393
[19] Ayala A P, Olivera M A S, Gesland J Y and Moreira R L 1998 *J. Phys.: Condens. Matter* **10** 5161
[20] Boulma E, Jouart J P, Bouffard M and Diaf M 2006 *J. Physique* IV at press
[21] Gesland J Y 1984 *PhD Thesis* University of Maine, France
[22] Couto dos Santos M A, Antic-Fidancev E, Gesland J Y, Krupa J C, Lemaître-Blaise M and Porcher P 1998 *J. Alloys Compounds* **275–277** 435
[23] Bouffard M, Duvaut T, Jouart J P, Khaidukov N M and Joubert M F 1999 *J. Phys.: Condens. Matter* **11** 4775
[24] Morrisson C A, Wortman D F, Leavitt R P and Jenssen H P 1980 *Gov. Rep. Announce US* **80** 2975
[25] Abdulsabirov R Y, Vinokurov A V, Ivanshin V A, Kurkin I N, Pudovik E A, Stolov A L and Yagudin S I 1987 *Opt. Spectrosc.* **63** 55
[26] Antic-Fidancev E, Lemaitre-Blaise M and Porcher P 1984 *Rare Earth Spectroscopy, Proc. Int. Symp. (Pub.1985)* p 134
[27] Diaf M, Boulma E and Chouahda Z 2003 *SPIE* **5036** 419